

## Different Pathways Are Involved in Arsenic-Trioxide-Induced Cell Proliferation and Growth Inhibition in Human Keratinocytes

X. Bi<sup>a</sup> J. Gu<sup>a</sup> Z. Guo<sup>a</sup> S. Tao<sup>a</sup> Y. Wang<sup>a</sup> L. Tang<sup>a</sup> J. Wu<sup>a</sup> Q. Mi<sup>b</sup>

<sup>a</sup>Department of Dermatology, Changhai Hospital, Second Military Medical University, Shanghai, PR China;

<sup>b</sup>Henry Ford Hospital Immunology Program, Department of Dermatology, Department of Medicine, Henry Ford Health System, Detroit, Mich., USA

### Key Words

Arsenic trioxide · Keratinocyte · Proliferation · Growth inhibition · Apoptosis

### Abstract

**Background:** Arsenic is a carcinogen that is associated with an increased risk of human skin cancer. On the other hand, arsenic trioxide (As<sub>2</sub>O<sub>3</sub>) has potential anticancer activity against a wide range of carcinomas. The mechanisms involved in these two opposing processes remain unclear. **Methods:** We used normal human keratinocytes (NHK), the human keratinocyte HaCaT cell line and human epidermal carcinoma cells (A431 cell line) to investigate potential pathways involved in the effects on cell proliferation and growth inhibition by different concentrations of As<sub>2</sub>O<sub>3</sub>. **Results:** At low concentrations (0.5–32 nM), As<sub>2</sub>O<sub>3</sub> enhanced keratinocyte proliferation and regulated the expression of about 172 genes. Among them, cell cycling pathway genes (including CDK4 and E2F1) were significantly upregulated. At high concentrations (0.5–10 μM), As<sub>2</sub>O<sub>3</sub> inhibited cell growth in NHK and HaCaT cells, but not in A431 cells. As<sub>2</sub>O<sub>3</sub> significantly induced NHK and HaCaT apoptosis through the activation of caspase-3, as well as cell cycle arrest at the G<sub>2</sub>–M phase. **Conclusion:** Our data suggest that different pathways are involved in As<sub>2</sub>O<sub>3</sub>-mediated proliferation and growth inhibition. In addition, skin carcinoma cells were resistant to

As<sub>2</sub>O<sub>3</sub>-induced cell growth inhibition and apoptosis when compared to NHK and HaCaT cells. Therefore, As<sub>2</sub>O<sub>3</sub> may not be appropriate for treatment of skin carcinomas.

Copyright © 2009 S. Karger AG, Basel

### Introduction

Epidemiological studies have shown a strong association between exposure to arsenic and an increased risk of tumors in the skin, lung, liver and prostate. Paradoxically, arsenic can also function as a chemotherapeutic agent in the treatment of relapsed or refractory acute promyelocytic leukemia [1–3]. In the past decade, several studies have identified possible mechanisms of arsenic carcinogenesis and anticancer effects, but the precise mechanisms remain unclear due to the lack of appropriate animal models. Studies in cultured cells have shown that low concentrations of arsenic compounds could stimulate the proliferation of vascular cells, epithelial cells and keratinocytes; this effect might be associated with increased expression of oxidative-stress-response genes, transcription factors such as AP-1, or members of the MAPK family [4–6]. Studies showing global alteration of gene expression in human keratinocytes by treatment with inorganic arsenic support these findings.

### KARGER

Fax +41 61 306 12 34  
E-Mail karger@karger.ch  
www.karger.com

© 2009 S. Karger AG, Basel  
1660–5527/10/0232–0068\$26.00/0

Accessible online at:  
www.karger.com/spp

Jun Gu and Qing-Sheng Mi  
Department of Dermatology, Changhai Hospital  
Second Military Medical University  
Shanghai 200433 (PR China)  
Tel. +86 21 8187 3318, Fax +86 21 2507 0622, E-Mail bixinling@163.com

As an effective chemotherapeutic agent for acute promyelocytic leukemia and some solid tumors, higher concentrations of  $As_2O_3$  can inhibit growth and induce apoptosis in a variety of cultured cells. Cellular events of arsenic-induced apoptosis have been associated with the redox status of thioredoxin-1 and cytochrome c, which facilitate mitochondrial permeability [7, 8]. In addition, the cell cycle and its regulation play an important role in arsenic-induced apoptosis. Some studies have shown that arsenic induces cell cycle arrest at the G2-M phase through the p21 signaling pathway in human fibroblasts [9]. Liao et al. [10] reported that arsenic induces human keratinocyte apoptosis by the FAS/FAS ligand pathway. Furthermore, some researchers hypothesized that  $As_2O_3$  could be used to treat head and neck squamous cell carcinomas [11]. However, no studies have been undertaken with 3 different types of keratinocytes in order to compare their sensitivity to arsenic treatment. In the present study, we investigated the biphasic effects of arsenic in keratinocytes.

## Materials and Methods

### Cell Lines and Culture

Normal human keratinocytes (NHK) were obtained from adolescent foreskin specimens, as previously described [12]. Isolated keratinocytes were cultured in keratinocyte serum-free medium (Invitrogen) with recombinant epidermal growth factor (0.2  $\mu$ g/ml) and bovine pituitary extract (20  $\mu$ g/ml). Cell lines HaCaT and A431 were maintained in Dulbecco's modified essential medium (Gibco/BRL) supplemented with 10% fetal calf serum (Life Technologies), 2 mM glutamine (Life Technologies) and 100 U/ml penicillin/streptomycin at 37°C in a humidified atmosphere containing 5%  $CO_2$ .

### Assessment of DNA Synthesis

HaCaT cells were seeded in 96-well plates at  $5 \times 10^3$ /well in complete media, and allowed to grow for an additional 24 h. Following a 24-hour starvation period in serum-free media, cells were then grown in media with various concentrations of  $As_2O_3$ . Eighteen hours later, cells in each well were labeled for 24 h with 1  $\mu$ Ci [ $^3H$ ]TdR. Cells were collected onto glass fiber filters, which were dried for 2 h. Incorporated radioactivity was counted in a liquid scintillation spectrometer, and the cultures were performed in triplicate.

### Microarray Analysis

HaCaT cells were continuously treated with 1 nM arsenic for 7 days, and total RNA was isolated using Trizol (Gibco/BRL); total RNA (30  $\mu$ g) was converted to cDNA probes by reverse transcription with oligo(dT) as primer. The cDNA probes were labeled with Cy3-dCTP for the control group and Cy5-dCTP for the treated group. The cDNA microarray, including 4,000 spots, was obtained from BioStar Genechip. The probes were denatured at

95°C for 2 min, and chilled on ice quickly. The cDNA microarrays were denatured in 95°C water for 30 s, and then placed into water-free ethanol. The denatured probes were added to region of the chip, and then sealed with a cover glass. The hybridization reaction lasted 18 h at 42°C. Then, cDNA microarrays were washed with 0.5% washing solution 1, followed by 0.5% washing solution 1 and 2% washing solution 2 for 10 min at 60°C, and then with 5% washing solution 3 for 10 min at 60°C. Chips were washed with 0.5% washing solution 1 again, and then dried at room temperature. All hybridization solutions and washing solutions were provided by BioStar Genechip. The cDNA microarray was scanned with ScanArray 4000 software, and the images were processed by GenePix 3.0 software. First, the values for Cy3 and Cy5 were obtained after background subtraction. Second, the adjusted value of Cy3 was obtained by multiplying ND by Cy3, and denoted as  $Cy3^*$ . Values of  $Cy3^*$  under 200 were replaced with 200. Finally, the  $Cy5/Cy3^*$  values for all genes were computed. Genes with a  $Cy5/Cy3^*$  ratio over 2 or under 0.5 were considered to be differentially expressed between the treated and control groups.

### Confirmation of Differential Expression by Semi-Quantitative RT-PCR

A semi-quantitative PCR protocol was employed to further confirm the cDNA microarray results. One-step RT-PCR (TaKaRa) was used. RNA was isolated as described above. One milligram of purified total RNA was used for each RT-PCR reaction. Primers designed for CDK4, E2F1 and  $\beta$ -actin were synthesized by Shanghai Sangon as follows: CDK4: 5' ATGTGGAGCGTTG-GCTGTATC 3', 5' TGGAGGCAATCCAATGAGATC 3', 114 bp; E2F1: 5'CACTGAATCTGACCACCAAGC 3', 5' CTCAGGGC-ACA GGAAAACATC 3', 509 bp;  $\beta$ -actin: 5' CCAGGCACCA-GGGCGTGAT 3', 5' TACTGGGTCTAGTACAAACT 3', 224 bp. PCR products were electrophoresed on 2% agarose gels and the gel images were captured and scanned using a Fluor-STM Multi-Imager (Bio-Rad).

### Cell Proliferation Inhibition Assay

$As_2O_3$  (Sigma) was dissolved in 0.1 M NaOH and diluted in 0.9% phosphate-buffered NaCl solution (PBS) to generate a 50-mM stock solution. In vitro growth inhibition of keratinocytes by  $As_2O_3$  was determined by measuring the MTT dye absorbance of living cells. Cells ( $10^4$ /well) were seeded in 96-well microtiter plates (Becton Dickinson), and were allowed to grow to 75% confluence. Cells were treated with 0, 0.38, 0.75, 1.5, 3, 6, 12 and 24  $\mu$ M  $As_2O_3$  for 24 and 48 h, then 20  $\mu$ l MTT (Sigma) solution (5 mg/ml in PBS) was added to each well, and the plates were incubated for an additional 4 h at 37°C. The supernatant was then aspirated. To achieve solubilization of the formazan formed in viable cells, 150  $\mu$ l DMSO was added to each well before measurement of the absorbance at 540 nm.

### Evaluation of Apoptosis

Cells were treated with 5  $\mu$ M  $As_2O_3$  for 24 h. Apoptotic cells were examined morphologically with light microscopy and electron microscopy. Apoptotic cells were also labeled with annexin V-FITC and propidium iodide for observation under a fluorescence microscope, and photomicrographs were taken with an integrated camera. In addition, apoptotic cells were also analyzed by FACS during the cell cycle analysis. Cells were classified as apoptotic if they exhibited sub-G1 DNA fluorescence and for-

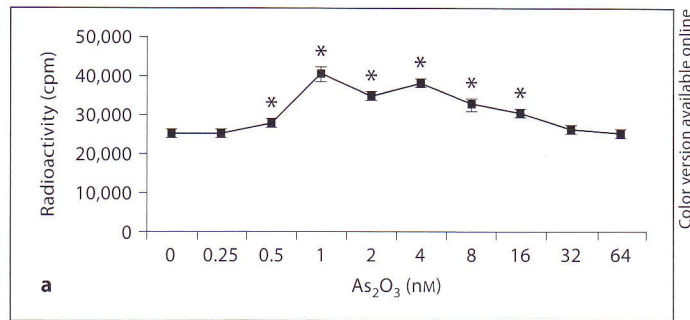
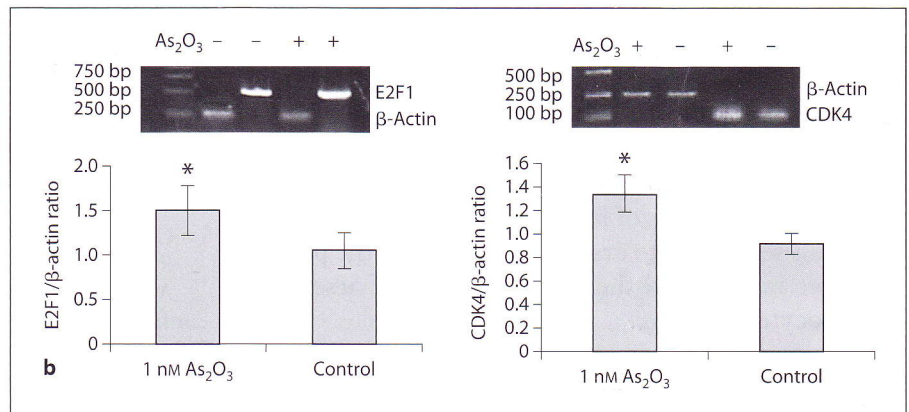


**Fig. 1.** Low concentrations of As<sub>2</sub>O<sub>3</sub> enhance keratinocyte proliferation. **a** HaCaT cells were grown in media with various concentrations of As<sub>2</sub>O<sub>3</sub>. Eighteen hours later, cells were labeled for 24 h with 1 μCi [<sup>3</sup>H]TdR. Incorporated radioactivity was counted in a liquid scintillation spectrometer, and cultures were performed in triplicate. \* p < 0.05 vs. baseline. **b** RT-PCR analysis confirmed that CDK4 and E2F1 were upregulated in HaCaT cells following As<sub>2</sub>O<sub>3</sub> treatment. Cells were treated with 1 nM As<sub>2</sub>O<sub>3</sub> for 7 days, and then the total RNA was analyzed by RT-PCR to determine the expression levels of CDK4 and E2F1.



ward-angle light scattering at the same or slightly lower intensity when compared to G1.

#### Cell Cycle Analysis

Cell cycle distribution was determined using Cycle Test™ PLUS DNA Reagent Kit (Becton Dickinson) according to the manufacturer's instructions. Arsenic-treated and control cells were trypsinized, and then stained with propidium iodide. The percentage of cells in the different phases of the cell cycle was measured with a FACSCalibur flow cytometer (Becton Dickinson), and analyzed by CELLQuest software.

#### Western Blot Analysis

After growth to 70–80% confluence, cells were treated with As<sub>2</sub>O<sub>3</sub> for the indicated times and concentration. Cells were then washed with cold PBS and lysed on ice for 30 min in lysis buffer. Protein concentrations were determined with a Bio-Rad protein assay kit. Total cellular protein (50 μg) was electrophoresed on 12% SDS polyacrylamide gels, and transferred to nitrocellulose membranes. Polyclonal antibodies against human caspase-3 and β-actin were used as the primary antibodies. Immunoblot analysis was carried out using a mouse IgG antibody coupled to horseradish peroxidase. Protein blots were visualized using an enhanced chemiluminescence kit (Amersham Bioscience).

#### Statistical Analysis

Statistical analyses were performed using SPSS software. All values are presented as means ± SD. ANOVA were performed when appropriate. Statistical significance was tested using Dunnett's test, and accepted at p < 0.05.

## Results

### CDK4 and E2F1 Are Involved in As<sub>2</sub>O<sub>3</sub>-Mediated Cell Proliferation

To obtain further evidence that low levels of As<sub>2</sub>O<sub>3</sub> exposure enhance keratinocyte proliferation, cells were examined by [<sup>3</sup>H]TdR incorporation assay. There was an initial stimulation of [<sup>3</sup>H]TdR incorporation into HaCaT cells at low concentrations (0.5–32 nM) of As<sub>2</sub>O<sub>3</sub>, as well as an inhibition of [<sup>3</sup>H]TdR incorporation when arsenic concentrations were increased (fig. 1a).

To elucidate the mechanisms by which As<sub>2</sub>O<sub>3</sub> enhances cell proliferation, gene expression in response to As<sub>2</sub>O<sub>3</sub> was evaluated by cDNA microarray. Microarray analysis showed that 172 genes were aberrantly expressed after arsenic exposure. Of these 172 genes, 57 were found to be upregulated and 115 were downregulated. These included genes encoding cell cycle regulators such as CDK4, as well as genes encoding growth factors and cytokines such as insulin-like growth factor-binding protein 4 and TNF superfamily member 4. Genes with altered expression also included signal transduction and transcription factors (table 1). The expression of the E2F1 transcription factor was increased 3.2-fold over the control, while CDK4 expression increased 3.5-fold. The CDK4-pRb

**Table 1.** List of differentially expressed genes in As<sub>2</sub>O<sub>3</sub>-treated HaCaT cells

Gene	Ratio	Definition	Modulation
Enzyme and enzyme regulatory genes			
NM_006367	0.450	adenylate cyclase-associated protein 1	↓
NM_004419	0.471	dual-specificity phosphatase 5 (DUSP5)	↓
NM_005857	2.189	zinc metalloproteinase	↑
NM_015205	2.260	ATPase, 11A	↑
NM_002396	2.326	malic enzyme 2 (ME2)	↑
M73047	2.465	tripeptidyl peptidase II	↑
BC002586	2.810	polymerase (RNA) III	↑
AF200478	0.304	protein serine/threonine phosphatase 4	↓
NM_000701	0.362	ATPase $\alpha$ 1	↓
AF102542	0.378	$\beta$ -1,6-N-acetylglucosaminyltransferase	↓
NM_014748	0.477	sorting nexin 17 (SNX17)	↓
NM_212482	0.498	fibronectin 1 (FN1)	↓
NM_005969	0.310	nucleosome assembly protein 1-like 4	↓
Structural molecule activity			
BC048198	0.404	$\alpha$ -2-HS-glycoprotein	↓
NM_015059	0.369	talin 2 (TLN2)	↓
Transcription factor			
BC050340	0.443	zinc finger protein 230	↓
NM_005524	0.455	hairy and enhancer of split 1	↓
NM_078628	2.014	male-specific lethal 3-like 1 (MSL3L1)	↑
AB209219	2.104	zinc finger protein 200 variant protein	↑
AF022158	2.562	KRAB domain zinc finger protein (ZFP37)	↑
NM_016271	2.963	ring finger protein 138 (RNF138)	↑
NM_005225	3.216	E2F transcription factor 1 (E2F1)	↑
NM_018179	2.179	ATF 7 interacting protein (ATF7IP)	↑
Cell adhesion molecules			
NM_000624	0.455	serine (or cysteine) proteinase inhibitor	↓
AB003592	2.084	neural adhesion molecule NB-3	↑
NM_0010123	2.090	opioid binding protein	↑
NM_033641	0.319	collagen, type IV, $\alpha$ 6 (COL4A6)	↓
Signal transduction-related genes			
NM_004625	0.455	WNT7A	↓
NM_012218	0.422	interleukin enhancer binding factor 3 (ILF3)	↓
NM_182470	0.431	pyruvate kinase, muscle (PKM2)	↓
BC000652	0.431	signal recognition particle	↓
BC035514	0.486	TEK tyrosine kinase, endothelial	↓
NM_021643	0.495	tribbles homolog 2 ( <i>Drosophila</i> ) (TRIB2)	↓
NM_003026	2.388	SH3-domain GRB2-like 2 (SH3GL2)	↑
AB209049	0.370	nucleoside-diphosphate kinase 7	↓
BC002352	0.403	Hsp40 homolog, subfamily B, member 1	↓
Apoptosis-associated genes			
NM_181861	0.490	apoptotic protease activating factor (APAF1)	↓
Receptor			
NM_175611	2.024	glutamate receptor, ionotropic, kainate 1	↑
NM_006667	2.123	progesterone receptor membrane component 1	↑
BC036030	2.163	gamma-aminobutyric acid (GABA) A receptor	↑
BC042897	2.186	nuclear receptor subfamily 2, member 2	↑
D26070	2.231	type 1 inositol 1,4,5-trisphosphate receptor	↑
BC017890	4.144	putative nucleic acid binding protein RY-1	↑
NM_002296	2.407	lamin B receptor (LBR)	↑
NM_173198	2.520	nuclear receptor subfamily 4A3 (NR4A3)	↑

**Table 1** (continued)

Gene	Ratio	Definition	Modulation
DNA-binding genes			
BC000459	0.433	polymerase delta 2, regulatory subunit	↓
NM_003286	0.403	topoisomerase (DNA) I (TOP1)	↓
NM_014321	0.497	origin recognition complex, subunit 6	↓
RNA-binding genes			
AB209403	0.429	iron-responsive element binding protein 2	↓
NM_006386	2.001	DEAD (Asp-Glu-Ala-Asp) box polypeptide 17	↑
Cytokine-related genes			
NM_003326	0.456	TNF superfamily, member 4 (TNFSF4)	↓
NM_001552	0.324	IGF binding protein 4 (IGFBP4)	↓
NM_007051	0.331	Fas (TNFRSF6) associated factor 1 (FAF1)	↓
NM_000584	0.331	interleukin 8 (IL8)	↓
Membrane protein			
AB209870	0.427	HLA class I histocompatibility antigen, E	↓
NM_005797	2.468	epithelial V-like antigen 1 (EVA1)	↑
NM_016447	2.636	membrane protein, palmitoylated 6 (MPP6)	↑
Tumor-related genes			
NM_182643	0.433	deleted in liver cancer 1 (DLC1)	↓
NM_004326	0.500	B-cell CLL/lymphoma 9 (BCL9)	↓
NM_001982	0.415	erb-b2 erythroblastic leukemia oncogene 3	↓
AB208831	0.413	v-raf murine sarcoma 3611 viral oncogene	↓
Metabolism-related genes			
NM_001969	2.108	eukaryotic translation initiation factor 5 (EIF5)	↑
AB013380	2.120	mono ATP-binding cassette protein	↑
AB209119	3.004	eukaryotic TIF 4 $\gamma$ , 3	↑
Cell cycle control genes			
NM_003550	2.211	MAD1 mitotic arrest deficient-like 1	↑
NM_000075	3.513	Cyclin-dependent kinase 4 (CDK4)	↑
Unknown			
NM_002973	0.419	ataxin 2 (ATXN2)	↓
NM_007192	2.123	suppressor of Ty 16 homolog ( <i>S. cerevisiae</i> )	↑
NM_000113	2.125	torsin family 1, member A (torsin A) (TOR1A)	↑
NM_018695	2.217	erbb2 interacting protein (ERBB2IP)	↑

pathway plays a significant role in cell cycle progression through the G1-S phase. E2F-1 is a transcription factor that is activated in the final stages of the Rb pathway. Overexpression of CDK4 and E2F1 observed by microarray after arsenic exposure was also confirmed by RT-PCR (fig. 1b).

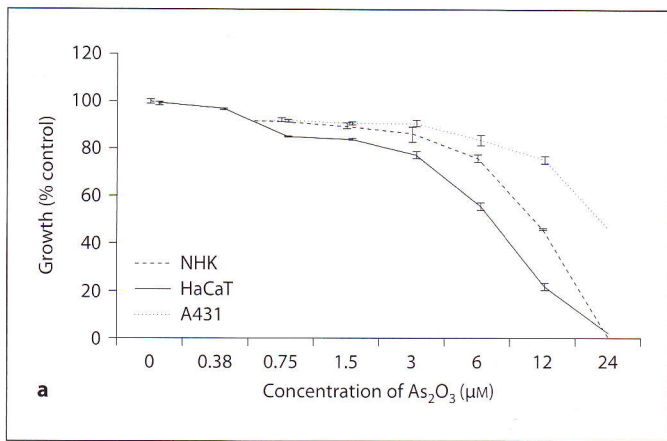
#### *As<sub>2</sub>O<sub>3</sub> Treatment Inhibited the Growth of NHK and HaCaT (but Not A431) Cells*

Previous reports have suggested that As<sub>2</sub>O<sub>3</sub> could induce tumor cell apoptosis from 3 to 5  $\mu$ M. Here, we tested whether As<sub>2</sub>O<sub>3</sub> could induce apoptosis in A341 skin tumor cells. As shown in figure 2a, there was a significant concentration-dependent inhibition of growth in NHK and HaCaT cells. The IC<sub>50</sub> values of As<sub>2</sub>O<sub>3</sub> for NHK cells

after 24 h incubation were about 10  $\mu$ M. In HaCaT cells, the concentration of As<sub>2</sub>O<sub>3</sub> required for 50% growth inhibition was about 6  $\mu$ M; the concentration required for 80% growth inhibition was about 10  $\mu$ M. However, As<sub>2</sub>O<sub>3</sub>-treated A431 cells did not show significant effects at concentrations less than 10  $\mu$ M. These results suggest that A431 cells were resistant to growth inhibition by arsenic when compared to NHK and HaCaT cells; thus, As<sub>2</sub>O<sub>3</sub> might not be suitable for treatment of skin tumors.

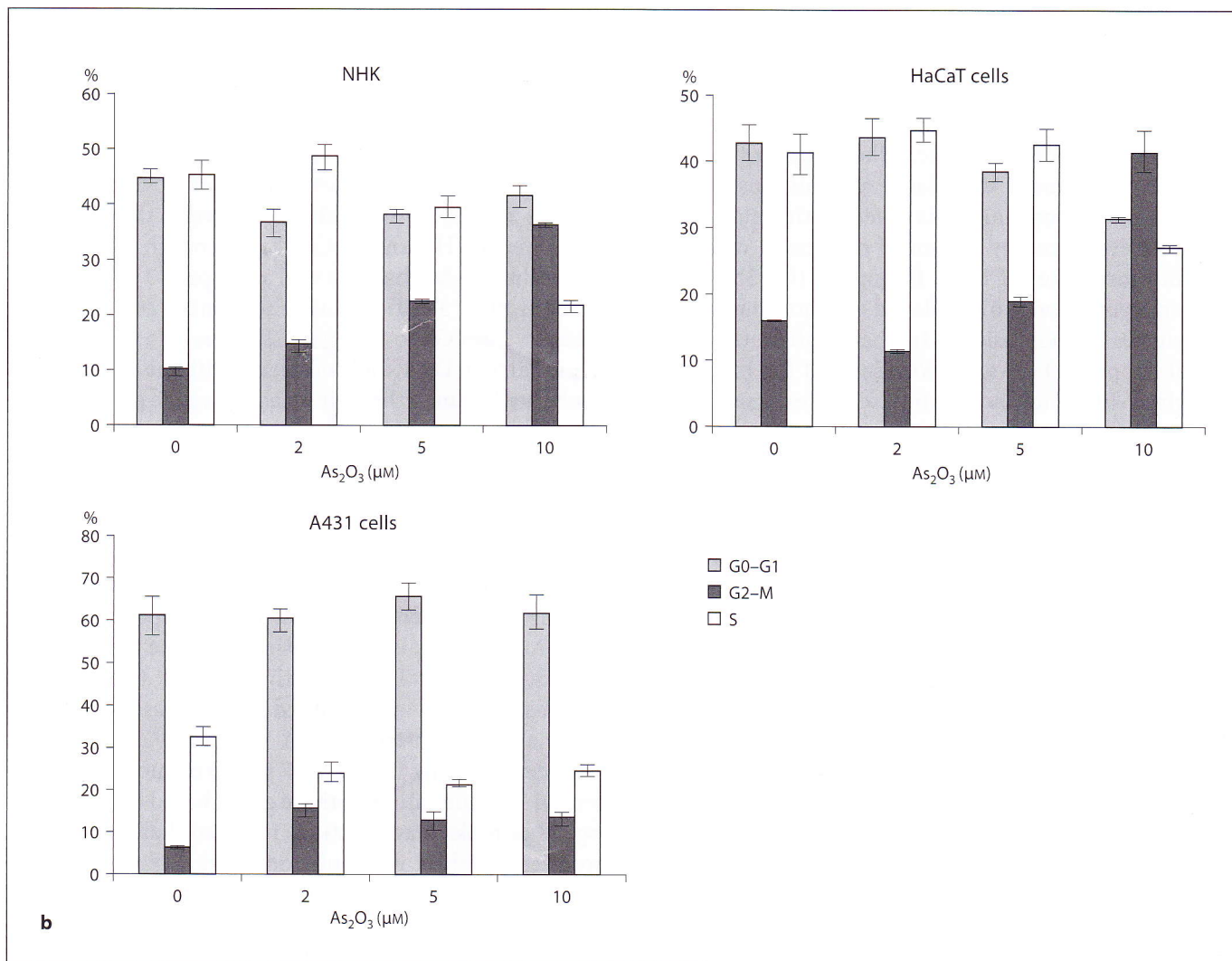
#### *As<sub>2</sub>O<sub>3</sub>-Induced G2-M Phase Arrest in NHK and HaCaT Cells*

To further define potential mechanisms involved in growth inhibition by As<sub>2</sub>O<sub>3</sub>, the effect of As<sub>2</sub>O<sub>3</sub> on the cell cycle was determined by FACS analysis. As shown in fig-



Color version available online

**Fig. 2. a** Effect of As<sub>2</sub>O<sub>3</sub> on the growth inhibition of NHK, HaCaT and A431 cell lines. Cell growth inhibition was assessed by MTT assay. Results represent means ± SD of 3 independent experiments with triplicate wells. **b** Flow cytometric analysis of cell cycle distribution in keratinocytes. Cells were cultured with medium alone and various concentrations of As<sub>2</sub>O<sub>3</sub> for 24 h as described in 'Materials and Methods'. Cell cycle distribution was analyzed by flow cytometry.



ure 2b, 3 independent experiments showed induction of an appreciable G2–M phase arrest in NHK and HaCaT cells following 24 h exposure to As<sub>2</sub>O<sub>3</sub>. In HaCaT cells, 18.94% of cells were arrested in the G2–M phase at 5 μM As<sub>2</sub>O<sub>3</sub> and 41.63% of cells at 10 μM; this was accompanied by a concomitant increase in the number of cells at the sub-G1 phase (fig. 3d). A similar pattern was observed for NHK cells. There was no significant change in cell cycle distribution for A431 cells following treatment with As<sub>2</sub>O<sub>3</sub>. Taken together, these results suggest that cell cycle arrest in the G2–M phase is a non-tumor-cell mechanism of growth inhibition by As<sub>2</sub>O<sub>3</sub>.

#### *As<sub>2</sub>O<sub>3</sub>-Induced Apoptosis in Keratinocytes*

Apoptosis induction is another possible mechanism for growth inhibition by As<sub>2</sub>O<sub>3</sub>. To test this, we analyzed apoptosis after As<sub>2</sub>O<sub>3</sub> treatment. Direct light microscopic examination of NHK and HaCaT cells revealed a concentration-dependent increase in the number of detached cells with condensed cytoplasm and nucleus (fig. 3a). Electron microscopic analysis revealed the late stage of apoptosis evidenced by advanced chromatin condensation and formation of DNA fragments (fig. 3b). At the same concentration, A431 cells did not show morphological features of apoptosis. To further confirm the induction of apoptosis by As<sub>2</sub>O<sub>3</sub>, we analyzed the binding of annexin V-FITC to phosphatidylserine exposed on the cell surface as an early marker of apoptosis in combination with propidium iodide. After treatment with 5 μM As<sub>2</sub>O<sub>3</sub> for 24 h, a greater number of NHK and HaCaT cells showed green fluorescence under fluorescence microscopy (fig. 3c). Using FACS analysis, we demonstrated that the proportion of apoptotic cells (sub-G1 phase) was increased in a concentration-dependent manner in NHK and HaCaT cells. There was no obvious change in sub-G1 phase distribution after exposure to 10 μM As<sub>2</sub>O<sub>3</sub> in A431 cells (fig. 3e).

#### *As<sub>2</sub>O<sub>3</sub>-Induced Apoptosis Is Related to Caspase-3 Activation*

It has been reported that several pathways are involved in As<sub>2</sub>O<sub>3</sub>-induced apoptosis [3, 10]. Caspase-3 is an apoptosis-promoting enzyme responsible for cleaving cellular substrates; this process leads to the characteristic alteration in cell morphology. As<sub>2</sub>O<sub>3</sub> treatment significantly induced caspase-3 activation in NHK and HaCaT cells in a concentration-dependent manner (fig. 4a, b). These results demonstrate that the underlying mechanism of As<sub>2</sub>O<sub>3</sub>-induced apoptosis in keratinocytes involves the activation of caspase-3.

## Discussion

In the present study, we investigated the effects of As<sub>2</sub>O<sub>3</sub> on cell growth as well as apoptosis and its signal transduction pathways in human keratinocytes. Consistent with previous reports, the current results indicate that As<sub>2</sub>O<sub>3</sub> has different effects on cell growth depending on its concentration [13, 14]. Recently, it has been found that arsenic might activate the EGFR–ERK pathway to induce gene expression and mitogenicity in several cell lines [6, 15]. Zhang et al. [13] reported that low concentrations of arsenite-promoted telomerase activity and increased telomere length, which corresponded with the induction of cell proliferation. However, high concentrations of arsenite decreased telomerase activity, telomere length and induced apoptosis. Here, we showed that low concentrations of As<sub>2</sub>O<sub>3</sub> can significantly enhance keratinocyte proliferation and regulate the expression of about 172 genes. Among these genes, CDK4 and E2F1 were significantly upregulated. In contrast, high concentrations of As<sub>2</sub>O<sub>3</sub>-induced cell growth inhibition and apoptosis in NHK and HaCaT cells through cell cycle arrest at the G2–M phase, as well as caspase-3 activation.

E2F1 plays a critical role in regulating cell cycle progression from G1 to S phase. E2F1 binds to its heterodimeric partner, DP-1, and complexes with the under-phosphorylated form of the retinoblastoma gene product pRb. During mid-to-late G1, after phosphorylation of pRb by cyclin D/CDK4, pRb dissociates from E2F1/DP-1, stimulating the transcription of genes necessary for G1–S phase transition [16, 17]. Several studies have suggested that overexpressed E2F1 protein could function as an oncogene product based on its ability to stimulate cell proliferation [18, 19]. CDK4 may also play an important role in this process. To gain more insight into the mechanisms of keratinocyte proliferation stimulated by a low concentration of As<sub>2</sub>O<sub>3</sub>, we examined gene expression changes using a cDNA microarray. A total of 172 genes were judged to be either induced (57 genes) or suppressed (115 genes). Categorization of these genes based on their biological or molecular functions revealed that they encode products involved in regulation of transcription, signal transduction, metabolism, cell cycle and cell adhesion. Cell cycle dysregulation has been implicated in the pathogenesis of most human cancers [20]. The CDK4–pRb pathway plays a particularly important role during cell cycle progression through the G1–S phase [21]. In this study, both E2F1 and CDK4 were significantly upregulated; this finding was confirmed by RT-PCR. Although genes associated with the MAPK pathway did not show

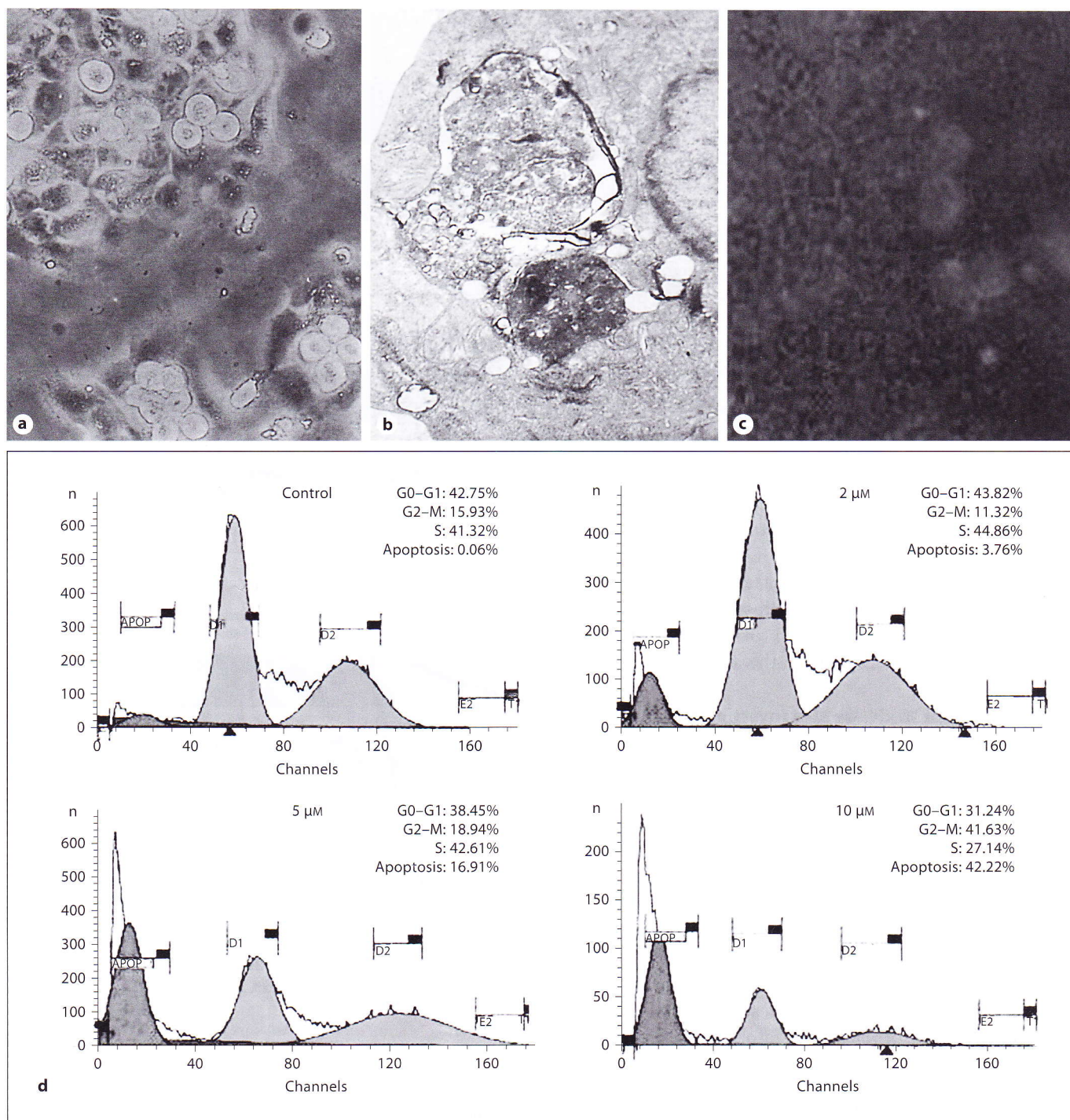


**Fig. 3.**  $As_2O_3$ -induced apoptosis in NHK and HaCaT, but not A431, cells. Cells were treated with 10  $\mu M$   $As_2O_3$  for 24 h. Morphological features of apoptosis were then observed and percentages of cells in the sub-G1 phase were analyzed by flow cytometry. **a** HaCaT cells.  $\times 200$ . **b** Electron microscopic findings of apoptotic NHK cells.  $\times 4,000$ . **c** Apoptotic HaCaT cells showed green fluorescence.  $\times 200$ . **d** Analysis of the sub-G1 phase showed concentration-dependent effects of  $As_2O_3$  on the induction of apoptosis in HaCaT cells.

total NHK cells.  $\times 4,000$ . **c** Apoptotic HaCaT cells showed green fluorescence.  $\times 200$ . **d** Analysis of the sub-G1 phase showed concentration-dependent effects of  $As_2O_3$  on the induction of apoptosis in HaCaT cells.

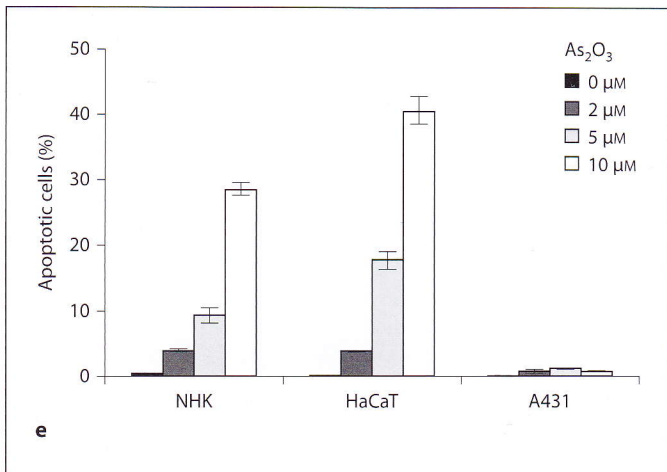


**Fig. 3. e** Comparison of the proportion of apoptotic cells in NHK, HaCaT and A431 cells using FACS analysis.

sharp upregulation on  $As_2O_3$  treatment, DUSP5 was significantly downregulated. Since DUSP5, a member of the dual-specificity protein phosphatase subfamily, negatively regulates members of the MAPK superfamily (MAPK/ERK, JNK, p38), downregulation of DUSP5 should lead to activation of the MAPK pathway in keratinocytes [22].

In the present study, we also investigated the effects of high concentrations of  $As_2O_3$  on growth inhibition in NHK, HaCaT and A431 cells.  $As_2O_3$  inhibited the growth of NHK and HaCaT cells (fig. 2a). The  $IC_{50}$  of  $As_2O_3$  was about 6–10  $\mu M$  in NHK and HaCaT cells, which was higher than that previously shown for hematopoietic cells [13, 23]. However, even at a higher concentrations (>10  $\mu M$ ),  $As_2O_3$  still only slightly inhibited the growth of A431 cells. Using flow cytometric analysis, we demonstrated that  $As_2O_3$  prominently induced G2–M phase arrest in NHK and HaCaT cells following 24 h of exposure when compared to A431 cells. These results were consistent with those of other investigators, who showed that the antiproliferative actions of arsenic were linked to G2–M phase arrest in U937 myeloid leukemia cells [23]. According to previous reports,  $As_2O_3$ -induced cell cycle arrest at the G1 and/or G2–M phase depends on the cell type [24]. Previous studies also showed that  $As_2O_3$ -induced G2–M phase arrest was accompanied by concentration-dependent decreases of cyclin A concomitant with reduced activity of CDK2-associated kinase [25]. Apoptosis induction is another possible mechanism for arsenic-induced growth inhibition. We showed that arsenic at 10  $\mu M$  induced apoptosis in NHK and HaCaT cells

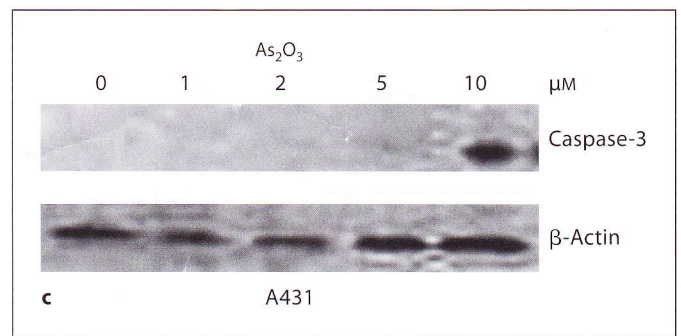
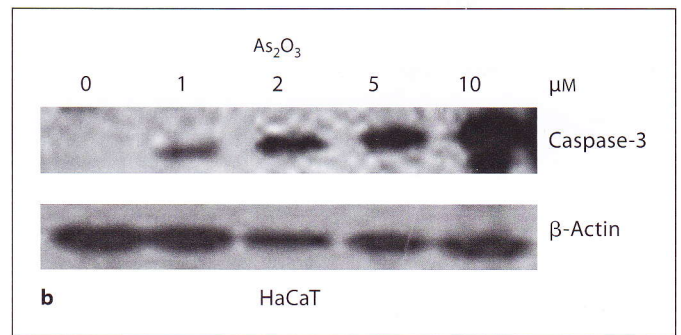
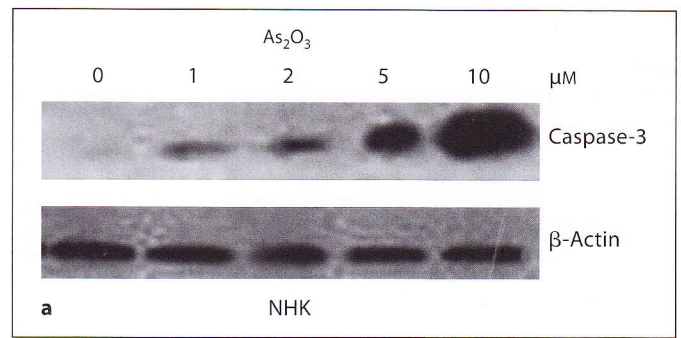


**Fig. 4.** Western blot analysis of caspase-3 expression in  $As_2O_3$ -treated keratinocytes. NHK, HaCaT and A431 cells were treated with different concentrations of  $As_2O_3$  for 24 h. Total cellular protein was subjected to Western blot analysis for the detection of caspase-3 as described in 'Materials and Methods'. Caspase-3 expression is shown in NHK (a), HaCaT (b) and A431 cells (c).

as evidenced by cell shrinkage, chromatin condensation and the appearance of annexin V staining (fig. 3a–c). The manifestations of apoptosis were consistent with a previous report [26]. However, no significant morphological changes were observed in A431 cells. Cell cycle analysis also revealed accumulation in the sub-G1 phase for NHK and HaCaT, but not A431, cells (fig. 3e). Thus, NHK and HaCaT cells were sensitive to arsenic-induced apoptosis, and A431 cells were more resistant. Chen et al. [27] reported that acute promyelocytic leukemia and B-cell

lymphoma cells were more sensitive to As<sub>2</sub>O<sub>3</sub>-induced apoptosis than other types of leukemia and lymphoma cells. It was suggested that this selectivity might partially be due to lower levels of cellular glutathione [28]. Many mechanisms have been proposed to be involved in As<sub>2</sub>O<sub>3</sub>-induced apoptosis, including production of reactive oxygen species, activation of caspase [11] and induction of JNK activity [3]. The caspase cascade is initiated by activation of caspase-8, which in turn induces activation of caspase-3. In our study, caspase-3 was activated in a concentration-dependent manner when NHK and HaCaT cells were exposed to As<sub>2</sub>O<sub>3</sub>, indicating the presence of cellular apoptosis. The result was consistent with the findings of Liao et al. [10], who showed that arsenic induces apoptosis in human keratinocytes by the FAS/FAS ligand pathway.

A recent study showed that a higher concentration (20 μM) of As<sub>2</sub>O<sub>3</sub> could upregulate p21 and induce toxicity in A431 cells [15]. Our results also suggest that a high level (20 μM) of arsenic would lead to significant toxicity in

NHK when compared to malignant epidermal cells. Therefore, clinical application of high concentrations of As<sub>2</sub>O<sub>3</sub> for treatment of squamous cell carcinoma may result in injury to normal tissues before any therapeutic effect can be observed. We therefore suggest caution when using arsenic to treat certain types of solid cancer, although recent studies have reported that As<sub>2</sub>O<sub>3</sub> has an antitumor effect in head and neck cancer [11]. In summary, our data indicate that, depending on the concentration, As<sub>2</sub>O<sub>3</sub> treatment can result in keratinocyte proliferation or apoptosis through different pathways. These results might help to explain the paradoxical carcinogenic and anticancer effects of arsenic.

### Acknowledgment

This work was supported by grants from the Basic Research Programs of Science and Technology Commission Foundation of Shanghai (No. 08JC1406800).

### References

- Cantor KP, Lubin JH: Arsenic, internal cancers, and issues in inference from studies of low-level exposures in human populations. *Toxicol Appl Pharmacol* 2007;222:252-257.
- Soignet SL, Maslak P, Wang ZG, Jhanwar S, Calleja E, Dardashti IJ, Corso D, DeBlasio A, Gabrilove J, Scheinberg DA, Pandolfi PP, Warrell RP: Complete remission after treatment of acute promyelocytic leukemia with arsenic trioxide. *New Engl J Med* 1998;339:1341-1348.
- Davison K, Mann KK, Waxman S, Miller WH Jr: JNK activation is a mediator of arsenic trioxide-induced apoptosis in acute promyelocytic leukemia cells. *Blood* 2004;103:3496-3502.
- Roybal CN, Hunsaker LA, Barbash O, Vander Jagt DL, Abcouwer SF: The oxidative stressor arsenite activates vascular endothelial growth factor mRNA transcription by an ATF4-dependent mechanism. *J Biol Chem* 2005;280:20331-20339.
- Drobná Z, Jaspers I, Thomas DJ, Stýblo M: Differential activation of AP-1 in human bladder epithelial cells by inorganic and methylated arsenicals. *FASEB J* 2003;17:67-69.
- Cooper KL, Myers TA, Rosenberg M, Chavez M, Hudson LG: Roles of mitogen activated protein kinases and EGF receptor in arsenite-stimulated matrix metalloproteinase-9 production. *Toxicol Appl Pharmacol* 2004;200:177-185.
- Tian C, Gao P, Zheng Y, Yue W, Wang X, Jin H, Chen Q: Redox status of thioredoxin-1 (TRX1) determines the sensitivity of human liver carcinoma cells (HepG2) to arsenic trioxide-induced cell death. *Cell Res* 2008;18:458-471.
- Bustamante J, Nutt L, Orrenius S, Gogvadze V: Arsenic stimulates release of cytochrome c from isolated mitochondria via induction of mitochondrial permeability transition. *Toxicol Appl Pharmacol* 2005;207:110-116.
- Yih LH, Lee TC: Arsenite induces p53 accumulation through an ATM-dependent pathway in human fibroblasts. *Cancer Res* 2000;60:6346-6352.
- Liao WT, Chang KL, Yu CL, Chen GS, Chang LW, Yu HS: Arsenic induces human keratinocyte apoptosis by the FAS/FAS ligand pathway, which correlates with alterations in nuclear factor-kappa B and activator protein-1 activity. *J Invest Dermatol* 2004;122:125-129.
- Seol JG, Park WH, Kim ES, Jung CW, Hyun JM, Lee YY, Kim BK: Potential role of caspase-3 and -9 in arsenic trioxide-mediated apoptosis in PCI-1 head and neck cancer cells. *Int J Oncol* 2001;18:249-255.
- Arakawa S, Hatano Y, Katagiri K, Terashi H, Fujiwara S: Effects of ultraviolet B irradiation on the production of regulated upon activation normal T-cell expressed and secreted protein in cultured human epidermal keratinocytes. *Arch Dermatol Res* 2006;297:377-380.
- Zhang TC, Schmitt MT, Mumford JL: Effects of arsenic on telomerase and telomeres in relation to cell proliferation and apoptosis in human keratinocytes and leukemia cells in vitro. *Carcinogenesis* 2003;24:1811-1817.
- Hwang BJ, Utti C, Steinberg M: Induction of cyclin D1 by submicromolar concentrations of arsenite in human epidermal keratinocytes. *Toxicol Appl Pharmacol* 2006;217:161-167.
- Liu ZM, Huang HS: As<sub>2</sub>O<sub>3</sub>-induced c-Src/EGFR/ERK signaling is via Sp1 binding sites to stimulate p21WAF1/CIP1 expression in human epidermoid carcinoma A431 cells. *Cell Signal* 2006;18:244-255.
- Xiao B, Spencer J, Clements A, Ali-Khan N, Mittnacht S, Broceño C, Burghammer M, Perrakis A, Marmorstein R, Gamblin SJ: Crystal structure of the retinoblastoma tumor suppressor protein bound to E2F and the molecular basis of its regulation. *Proc Natl Acad Sci USA* 2003;100:2363-2368.
- Martinsson HS, Starborg M, Erlandsson F, Zetterberg A: Single cell analysis of G1 check points - the relationship between the restriction point and phosphorylation of pRb. *Exp Cell Res* 2005;305:383-391.
- Zhang SY, Liu SC, Johnson DG, Klein-Szanto AJ: E2F-1 gene transfer enhances invasiveness of human head and neck carcinoma cell lines. *Cancer Res* 2000;60:5972-5976.

- 19 Salon C, Merdzhanova G, Brambilla C, Brambilla E, Gazzeri S, Eymin B: E2F-1, Skp2 and cyclin E oncoproteins are upregulated and directly correlated in high-grade neuroendocrine lung tumors. *Oncogene* 2007;26:6927–6936.
- 20 Kim Y, Shintani S, Kohno Y, Zhang R, Wong DT: Cyclin G2 dysregulation in human oral cancer. *Cancer Res* 2004;64:8980–8986.
- 21 Kusume T, Tsuda H, Kawabata M, Inoue T, Umesaki N, Suzuki T, Yamamoto K: The p16-cyclin D1/CDK4-pRb pathway and clinical outcome in epithelial ovarian cancer. *Clin Cancer Res* 1999;5:4152–4157.
- 22 Mandl M, Slack DN, Keyse SM: Specific inactivation and nuclear anchoring of extracellular signal-regulated kinase 2 by the inducible dual-specificity protein phosphatase DUSP5. *Mol Cell Biol* 2005;25:1830–1845.
- 23 McCollum G, Keng PC, States JC, McCabe MJ Jr: Arsenite delays progression through each cell cycle phase and induces apoptosis following G2/M arrest in U937 myeloid leukemia cells. *J Pharmacol Exp Ther* 2005;313:877–887.
- 24 Park WH, Seol JG, Kim ES, Hyun JM, Jung CW, Lee CC, Kim BK, Lee YY: Arsenic trioxide-mediated growth inhibition in MC/CAR myeloma cells via cell cycle arrest in association with induction of cyclin-dependent kinase inhibitor, p21, and apoptosis. *Cancer Res* 2000;60:3065–3071.
- 25 Woo SH, Park MJ, An S, Lee HC, Jin HO, Lee SJ, Gwak HS, Park IC, Hong SI, Rhee CH: Diarsenic and tetraarsenic oxide inhibit cell cycle progression and bFGF- and VEGF-induced proliferation of human endothelial cells. *J Cell Biochem* 2005;95:120–130.
- 26 Zhu QX, Shen T, Tu DY, Ding R, Liang ZZ, Zhang XJ: Protective effects of *Ginkgo biloba* leaf extracts on trichloroethylene-induced human keratinocyte cytotoxicity and apoptosis. *Skin Pharmacol Physiol* 2005;18:160–169.
- 27 Chen D, Chan R, Waxman S, Jing Y: Buthionine sulfoximine enhancement of arsenic trioxide-induced apoptosis in leukemia and lymphoma cells is mediated via activation of c-Jun NH2-terminal kinase and up-regulation of death receptors. *Cancer Res* 2006;66:11416–11423.
- 28 Yang CH, Kuo ML, Chen JC, Chen YC: Arsenic trioxide sensitivity is associated with low level of glutathione in cancer cells. *Br J Cancer* 1999;81:796–799.